

Closed-loop System Identification of Wind Turbines in the Presence of Periodic Effects

Gijs van der Veen*

G.J.vanderVeen@tudelft.nl

Jan-Willem van Wingerden

J.W.vanWingerden@tudelft.nl

Michel Verhaegen

M.Verhaegen@tudelft.nl

Delft Center for Systems and Control, Delft University of Technology, Delft, The Netherlands

Abstract

The use of trailing edge flaps has developed into a promising technique to reduce loads on large wind turbines. Fatigue and extreme loads, predominantly in the blade root, are critical to the life of rotor blades and these loads can be reduced significantly by locally influencing the lift along the span of the rotor blades. To design controllers for such “smart” rotor systems, linear models are still the tool of choice. Although linear models can be obtained from the first principles models implemented in aeroelastic design tools, we emphasize the value of system identification techniques. Identification of linear models of wind turbine dynamics is complicated by the fact that strong periodic components are present in output measurements. These components are associated with effects such as gravity, wind shear, skew inflow conditions, tower shadow and rotational sampling of the turbulent wind field. When traditional system identification techniques are used, the estimates may be very poor due to the strong presence of these components in the measurements. In this paper, a subspace identification method is described together with a method to remove the effect of periodic disturbances on the quality of identified models, by generating periodic signals that serve as additional inputs to the identification procedure. The paper is concluded with an example that demonstrates the effectiveness of the suggested approach.

Keywords: System identification, subspace identification, periodic disturbances, MOESP, smart rotor

1 Introduction

The use of trailing edge flaps has developed into a promising solution to reduce loads in large wind turbines. Fatigue loads, predominantly in the blade root, are critical to the life of rotor blades and these loads can be reduced significantly by locally influencing the lift along the span of the rotor blades. This issue will become even more important as rotor sizes increase beyond

150 m. Since the pioneering research on trailing edge flaps [1, 2, 3, 4] which emerged from the field of rotorcraft research [5, 6, 7], several proofs of concept, both computational and experimental, have demonstrated the potential for load reduction using distributed flap actuation [4, 8, 9, 10]. Extending fatigue life by reducing dynamic loads is an important factor in lowering the cost of energy and supporting the trend of increasingly large rotors. To design controllers for wind turbines or their subsystems, linear models are still widely used due to their simplicity and the wide range of tools available [11, 12, 13, 14]. Although linear models can be obtained from the first principles models implemented in aeroelastic design tools, we emphasize the value of system identification techniques. Often, linearised models obtained from first-principles models are of high order such that a reduction step may be necessary. Furthermore, such models follow the theoretical nature of the model and therefore parameters are bound to differ from the true turbine’s parameters [15]. A linear model obtained from measurements of a true system provides a realistic model of the underlying dynamics which, in many cases, gives a more accurate or relevant dynamical description of the process under consideration [16, 17]. Identification of linear models of wind turbine dynamics is complicated by the fact that strong periodic components are present in the measurements of certain output channels. These components are associated with effects such as gravity, wind shear, skew inflow conditions, tower shadow and rotational sampling of the turbulent wind field. These loads that arise during operation are highly correlated with the rotor speed and its higher harmonics. When standard system identification methods are applied, the estimates may be very poor due to the strong presence of these components in the measurements. Several authors have studied system identification problems in the presence of periodic disturbances. In [18], the authors extend a subspace identification framework to incorporate periodic disturbances. Unfortunately, the frequency of the disturbance must be constant, and its period must span an integer number of data samples. The same authors also propose a method to deal with arbitrary periodic disturbances [19], but at present there are no provisions for closed-loop data or

*The authors gratefully acknowledge the support of Vestas Wind Systems A/S.

the presence of (coloured) process noise. In this paper, we revisit an idea suggested by Van Baars et al. [20] and propose the use of periodic signals with the same frequency as the rotor and its higher harmonics as additional inputs to the identification problem. This method is simple to implement in practice and since the additional signals only contain power at a few isolated frequencies, the identified dynamics are not affected by this procedure. Experimental results demonstrate a significant improvement of estimated models when this technique is used. The technique is also applicable to closed-loop identification problems.

The paper is structured as follows: In section 2 the advantages of a system identification approach are highlighted. In section 3 the basic principles of subspace identification are discussed. In section 4 a procedure is described to deal with periodic disturbances. In section 5 the methodology is applied to the example of a “smart” rotor. The paper concludes with a discussion of the results and some recommendations for further work.

2 Advantages of system identification

It is common practice to tune the controllers in present-day turbines on the basis of linear system models. Usually, such models are obtained from first principles models implemented in aeroelastic codes, which are then numerically linearised in one or more operating points. Although such procedures yield the desired linear models, these inherently exhibit dynamics that are different from the true system due to the theoretical and approximative nature of the simulation tools [15]. Also, the resulting models may be of high order, especially in the case of blade element momentum models. While it is very beneficial to have access to simulation tools during the design of wind turbines, it is also relevant to be able to obtain models from measured operational data that describe the process under control more accurately. This is relevant when identifying (sub)systems of a wind turbine that can only operate safely or within reasonable limits when operating in closed-loop [17]. Furthermore, it is well known that measuring the system under closed-loop operation provides more accurate linear models if such models are used for control design purposes [17, 21, 22]. That is, the closed-loop displays better performance if the controller is designed on the basis of such linear models.

3 Subspace identification framework

The identification framework used in this research is based on the subspace class of identification methods [23]. These methods seek a linear time-invariant state-space model of the system to be identified based on matrices constructed from input-output data. The fun-

damental subspaces associated with these matrices can be exploited to find an approximate realization of the data-generating system. This system can be retrieved in a state-space form. More specifically, the Multivariable Output-Error State-space (MOESP) method is applied to find the system matrices $\{A, B, C, D\}$ that define the identified model. A key advantage of subspace methods is that they are based on efficient linear least-squares techniques and therefore non-iterative in nature. As such, they result in a globally optimal solution for a given model order in a single step. Furthermore, the size of the data matrices and the model order are the only decision parameters, making the method simpler to use than most prediction-error methods which may require an a priori parametrisation and a non-linear least-squares optimisation. The method can deal with an arbitrary number of inputs and outputs and can therefore identify MIMO systems. In light of the previous section, it should be noted that the method applied here is also suited to closed-loop identification problems where knowledge of the controller operating in the closed-loop is not required. This novel extension of the MOESP algorithm (CL-MOESP) has been treated in detail in [24].

3.1 Elements of subspace identification

For simplicity of presentation, we only present the basic elements of MOESP subspace identification. For a complete treatment, the reader is referred to [23]. An extension to the case of closed-loop identification with additional periodic signals is treated in [24].

In the framework of subspace identification, a linear dynamic relation is estimated (typically in state-space format) between the subspaces of matrices constructed from input and output data $\{u_k, y_k\}_{k=1}^N$. That is, a linear model of the following form is to be identified:

$$x_{k+1} = Ax_k + Bu_k, \quad (1a)$$

$$y_k = Cx_k + Du_k, \quad (1b)$$

with $A \in \mathbb{R}^{n \times n}$, $B \in \mathbb{R}^{n \times m}$, $C \in \mathbb{R}^{l \times n}$ and $D \in \mathbb{R}^{l \times m}$. Additionally, $x_k \in \mathbb{R}^n$, $u_k \in \mathbb{R}^m$ and $y_k \in \mathbb{R}^l$ are respectively the state vector, input signal and output signal. In this presentation it is assumed that noise does not affect the system, but this hypothetical assumption is not made in the full treatment. In the next sections it will be shown how a dynamic model can be obtained from the measured input and output data sets.

3.2 Deriving the data equations

Starting from some initial state x_k , the state equation can be propagated j steps ahead, resulting in the expression

$$x_{k+j} = A^j x_k + \begin{bmatrix} A^{j-1}B & \cdots & AB & B \end{bmatrix} \begin{bmatrix} u_k \\ \vdots \\ u_{k+j-1} \end{bmatrix}$$

Based on this equation and the output equation (Eq. 1b) future outputs can then be written as

$$y_{k+j} = CA^j x_k + \begin{bmatrix} CA^{j-1}B & \cdots & CAB & CB & D \end{bmatrix} \begin{bmatrix} u_k \\ \vdots \\ u_{k+j-1} \\ u_{k+j} \end{bmatrix}$$

Stacking s of these predicted outputs results in Eq. 2.

$$\begin{bmatrix} y_k \\ y_{k+1} \\ \vdots \\ y_{k+s-1} \end{bmatrix} = \mathcal{O}_s x_k + \mathcal{H}_s \begin{bmatrix} u_k \\ u_{k+1} \\ \vdots \\ u_{k+s-1} \end{bmatrix}, \quad (2)$$

where the block-Toeplitz matrix \mathcal{H}_s is defined as

$$\mathcal{H}_s = \begin{bmatrix} D & 0 & 0 & \cdots & 0 \\ CB & D & 0 & \ddots & 0 \\ CAB & CB & D & \ddots & 0 \\ \vdots & & & \ddots & \ddots \\ CA^{s-2}B & CA^{s-3}B & \cdots & CB & D \end{bmatrix}.$$

The extended observability matrix is also recognised in Eq. 2;

$$\mathcal{O}_s = \begin{bmatrix} C \\ CA \\ \vdots \\ CA^{s-2} \end{bmatrix}. \quad (3)$$

The data columns in Eq. 2 can be augmented with time-shifted versions. To this end, Hankel matrices of input and output data are defined as follows, assuming that all samples at our disposal are used:

$$Y_{1,s,N} = \begin{bmatrix} y_1 & y_2 & \cdots & y_{N-s+1} \\ y_2 & y_3 & \cdots & y_{N-s+2} \\ \vdots & \vdots & \ddots & \vdots \\ y_s & y_{s+1} & \cdots & y_N \end{bmatrix},$$

$$U_{1,s,N} = \begin{bmatrix} u_1 & u_2 & \cdots & u_{N-s+1} \\ u_2 & u_3 & \cdots & u_{N-s+2} \\ \vdots & \vdots & \ddots & \vdots \\ u_s & u_{s+1} & \cdots & u_N \end{bmatrix}.$$

The integer s denotes the number of block rows in the Hankel matrices. s should be chosen to be about 2-3 times the maximum expected model order. The data equation incorporating all measurement data can now be given as follows:

$$Y_{1,s,N} = \mathcal{O}_s X_{0,N} + \mathcal{H}_s U_{1,s,N}, \quad (4)$$

where $X_{0,N} = [x_1 \ \cdots \ x_{N-s+1}]$ represents the *state sequence*. Note that the state sequence is at this point

unknown so that it is not possible yet to solve this system for the unknown parameters. In the next section, a projection matrix will be found that eliminates the influence of the input on the system, so that the unforced response (response to the initial state) can be found.

3.3 Estimating the extended observability matrix \mathcal{O}_s

In Eq. 4 the matrix $U_{1,s,N}$ is known. Therefore, a projection matrix

$$\Pi_{U_{1,s,N}}^\perp = I - U_{1,s,N}^\top (U_{1,s,N} U_{1,s,N}^\top)^{-1} U_{1,s,N}$$

can be constructed, such that $U_{1,s,N} \Pi_{U_{1,s,N}}^\perp = 0$. This matrix eliminates $U_{1,s,N}$ from the right hand side of Eq. 4 resulting in

$$Y_{1,s,N} \Pi_{U_{1,s,N}}^\perp = \mathcal{O}_s X_{0,N} \Pi_{U_{1,s,N}}^\perp. \quad (5)$$

This equation provides the projection of the output Hankel matrix $Y_{1,s,N}$ onto the orthogonal complement of the row space of the input Hankel matrix. If the input Hankel matrix has full row rank¹, it can be shown that the column space of \mathcal{O}_s is contained in and, in fact, equal to the column space of $Y_{1,s,N} \Pi_{U_{1,s,N}}^\perp$ [23]:

$$\text{range}(\mathcal{O}_s) = \text{range}(Y_{1,s,N} \Pi_{U_{1,s,N}}^\perp). \quad (6)$$

Thus, the column-space of $Y_{1,s,N} \Pi_{U_{1,s,N}}^\perp$ serves as a basis for the column space of the extended observability matrix \mathcal{O}_s . This column space can be found by performing a singular value decomposition of R_{22} , which yields

$$Y_{1,s,N} \Pi_{U_{1,s,N}}^\perp = U_n \Sigma_n V_n^\top, \quad (7)$$

where n is the number of non-zero singular values and also the order of the underlying dynamical system. The columns of U_n provide a basis for \mathcal{O}_s so that $\mathcal{O}_s = U_n$ up to a similarity transformation. In the case of noise affecting the measurements, all of the singular values will be non-zero, but a gap between two successive singular values will often indicate the order of the system. In such cases, instrumental variables [23] need to be used to obtain unbiased estimates of the system matrices.

Estimates of the matrices A and C can subsequently be found by examining the structure of Eq. 3. Given the structure of \mathcal{O}_s , the C -matrix is found as the first l rows of \mathcal{O}_s . A can be found as the solution to the overdetermined problem $\mathcal{O}_s(1 : (s-1)l, :)A = \mathcal{O}_s(l+1 : sl, :)$ (using MATLAB notation). The matrices B and D and the initial state x_0 can be computed by solving a least-squares problem as shown in the next section.

¹Note that this is equivalent to requiring that the individual inputs are persistently exciting of at least order s [23]

3.4 Estimating B , D and the initial state

Based on the system equations (Eq. 1), the output at time k can be written as as

$$y_k = CA^k x_0 + \sum_{\tau=0}^{k-1} CA^{k-\tau-1} Bu_{\tau} + Du_k$$

Since A and C are now known, it can be seen that the unknown elements of $x(0)$, B and D appear linearly. Therefore, the parameters can be obtained after solving a least-squares problem [23]. An efficient method is described in [24].

3.5 Experiment design

To be able to identify a suitable model from input-output data, several guidelines must be observed [23, 25]. The excitation signal should be such that it excites all the relevant modes of the system. At the same time, the excitation signal should observe the system's limitations, yet provide sufficient excitation to result in a satisfactory signal-to-noise ratio. Common identification signals are broadband multisine signals, step signals and pseudo-random binary sequences. The latter type has the advantage of being strictly limited in amplitude, while delivering maximal signal energy to the system within the amplitude constraints. Furthermore, if such a sequence is sampled at fraction of the system sample rate, the excitation spectrum can be shaped such that the low-frequency content is emphasised without violating amplitude constraints. In cases where severe noise affects the system, which might occur with high turbulence levels in wind energy, the only means of achieving a satisfactory signal-to-noise ratio may be to use a crested multisine signal containing a limited number of strategically chosen frequencies. In general, a model identification procedure is an iterative procedure, in which more knowledge of the system's underlying dynamics is gained after every trial. This knowledge can be exploited to tailor the excitation and measurement conditions in subsequent steps. Generally, the sample rate should be up to about ten times the bandwidth of interest to avoid effects of aliasing and at the same time limit the amount of high-frequency noise that contaminates the measurements [25]. At the same time, the experiment duration should usually be at least about ten times the length of the slowest time constant of the system to ensure that the low-frequency behaviour of the process is captured. It is clearly seen that a trade-off between sample frequency and measurement duration must be made that is dictated by storage and/or processing limitations regarding the number of data points. The duration is further constrained by the ability for the process to operate around one operating point in the case of a non-linear system.

4 Embedding periodic disturbances into the identification framework

The identification of blade dynamics subject to control devices such as trailing edge flaps is complicated by several issues. First, on real turbines actuator deflections and rates are limited, while at the same time strong disturbances are present. This can make it hard to achieve satisfactory signal-to-noise ratios for system identification procedures. Furthermore, a significant part of the disturbances are periodic in nature and highly correlated with the periodic motion of the rotor (1P, 2P, 3P, etc...). These periodic disturbances are mainly associated with effects such as gravity, wind shear, skew inflow conditions, tower shadow and rotational sampling of the turbulent wind field. Such strong periodic components fail to match the standard hypothesis in system identification that measurements are corrupted with a stochastic noise component.

Since the output measurements (e.g. tip displacement or blade root moment) are highly influenced by the periodic disturbances, the standard identification procedures are likely to search for a causal relation between the applied inputs and the outputs which is not present at the frequencies of the periodic disturbances. In many cases this will lead to a poor description of the input-to-output behaviour of the system. In this paper we make use of the knowledge of the rotor speed and propose to add signals to the identification procedure to reduce the effect of this problem.

Since the output measurements are to a large extent corrupted with periodic signals of known frequencies, it is possible to construct virtual input signals with corresponding frequencies that are able to account for periodic components in the outputs [20]. The operation of such signals can be explained as follows: the outputs are affected by a periodic signal of unknown amplitude and phase. Any periodic sinusoidal signal of unknown amplitude and phase can be constructed from a linear combination of a cosine and sine function with unit amplitude and zero phase:

$$A \sin(\omega t + \phi) = \alpha \sin \omega t + \beta \cos \omega t \quad (8)$$

Thus, pairs of sine and cosine input signals can be generated at each of the disturbance frequencies, to account for the periodic components in the output. As shown in Figure 1, these constructed signals can be added as inputs to the identification procedure together with the actual inputs applied to the system. One has to take care when adding periodic signals as inputs as they contain energy at only one frequency. Usually, a standard assumption in system identification is that each of the input signals has a fairly broad-band spectrum to ensure that the numerical operations remain well-conditioned. To deal with the narrow-band inputs, the subspace algorithm had to be modified to avoid solving a rank-deficient

least-squares problem. This modification is treated in detail in [24].



Figure 2: “Smart” rotor scale model in the Open Jet facility.

5 Results for a “smart” rotor blade

Recently, measurements were performed on a scale model of a wind turbine [26] in the Open Jet wind tunnel at Delft University of Technology (Fig. 2). The scale model has two “smart” rotor blades, where each of the blades is equipped with piezoelectric trailing edge flaps. These devices are used to alleviate the blade loads by modifying the the local aerodynamic loads. The aforementioned identification procedure was used to identify linear state-space models of the system to support controller design and improve understanding of the dynamics. The case under consideration concerned the identification of the dynamics from the trailing edge flap actuators on each of the two blades to the strain measurements in the root of the blades. The strains are measured using piezoelectric macro fibre composite (MFC) strain gauges. In an experiment, 10000 samples of I/O data were obtained at a rate of 100 Hz. As input signals two independent pseudo-random binary sequences were used with amplitudes of 400 V, close to the saturation limits, and a sample rate of 50 Hz (half the sample frequency) to increase energy in the low-frequency excitation region. To determine the problematic periodic components, the power spectra of the output signals were analysed. These showed distinct peaks at 1P and 3P frequencies. Figure 3 shows how the periodic components affect the output measurements: the excitation capability of the actuators is limited and therefore the strong components at 1P and 3P are still strongly represented in the output measurements and cannot be dominated by the actuation. Since turbulence was hardly present under these experimental conditions, the random input signal proved able to excite the system to a sufficient extent apart from the frequencies where periodic effects dominate the response. In Figure 4, the results of an identification experiment are shown. The strong effect of

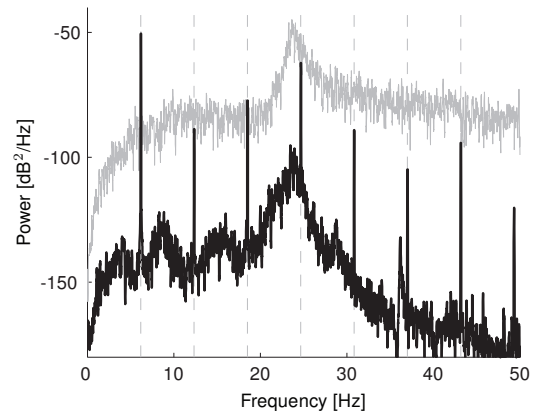


Figure 3: Output spectra for measurements with (—) and without (—) an excitation signal present, showing the dominance of the periodic effects at 1P and 3P.

the periodic signals on the output measurements forces the identification procedure to identify incorrect dynamics specifically at the 1P and 3P frequencies to account for the presence of these frequencies in the output signal. With the addition of periodic signals as indicated above, these incorrect dynamics are no longer present. In Figure 5 the bode magnitude diagram of the complete 12th order model is shown. The identified models have been used successfully in a model based feed-forward-feedback control design which was applied to the “smart” rotor model [27].

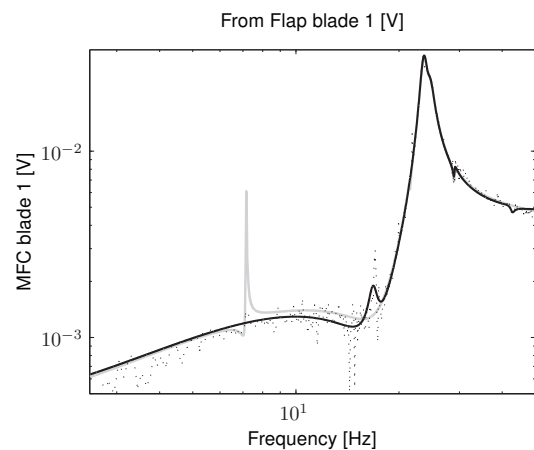


Figure 4: Comparison of two linear models from one the trailing edge actuators to a strain measurements at the blade root showing the mismatch at 1P resulting from a standard identification procedure. The grey line (—) corresponds to the identified model without adding periodic input signals, the black line (—) corresponds to identified model obtained with added periodic signals. The results shown correspond to the case $\omega = 430$ rpm and $v = 10$ m/s.

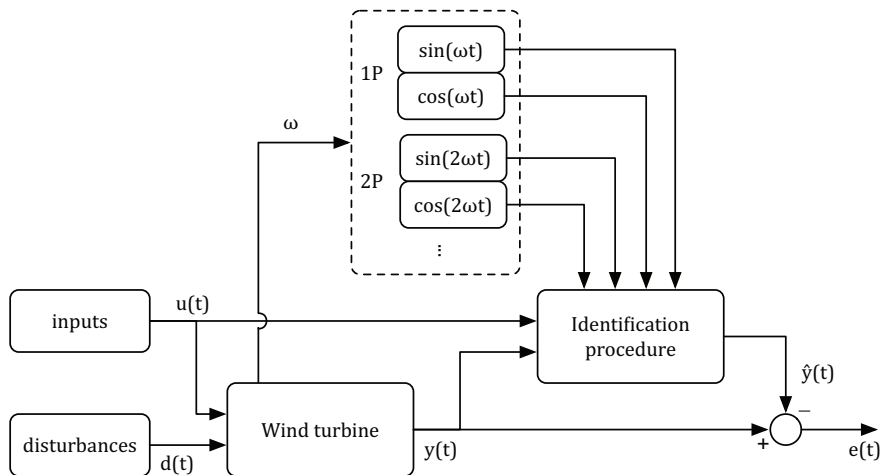


Figure 1: The identification setup used in this context. The measured identification data $y(t)$ is perturbed by unknown disturbances $d(t)$ acting on the turbine; the 1P and 2P periodic signals are added to the set of input signals $u(t)$ used for identification in order to suppress the effect of the disturbances on the quality of the identified model of $u(t) \rightarrow y(t)$.

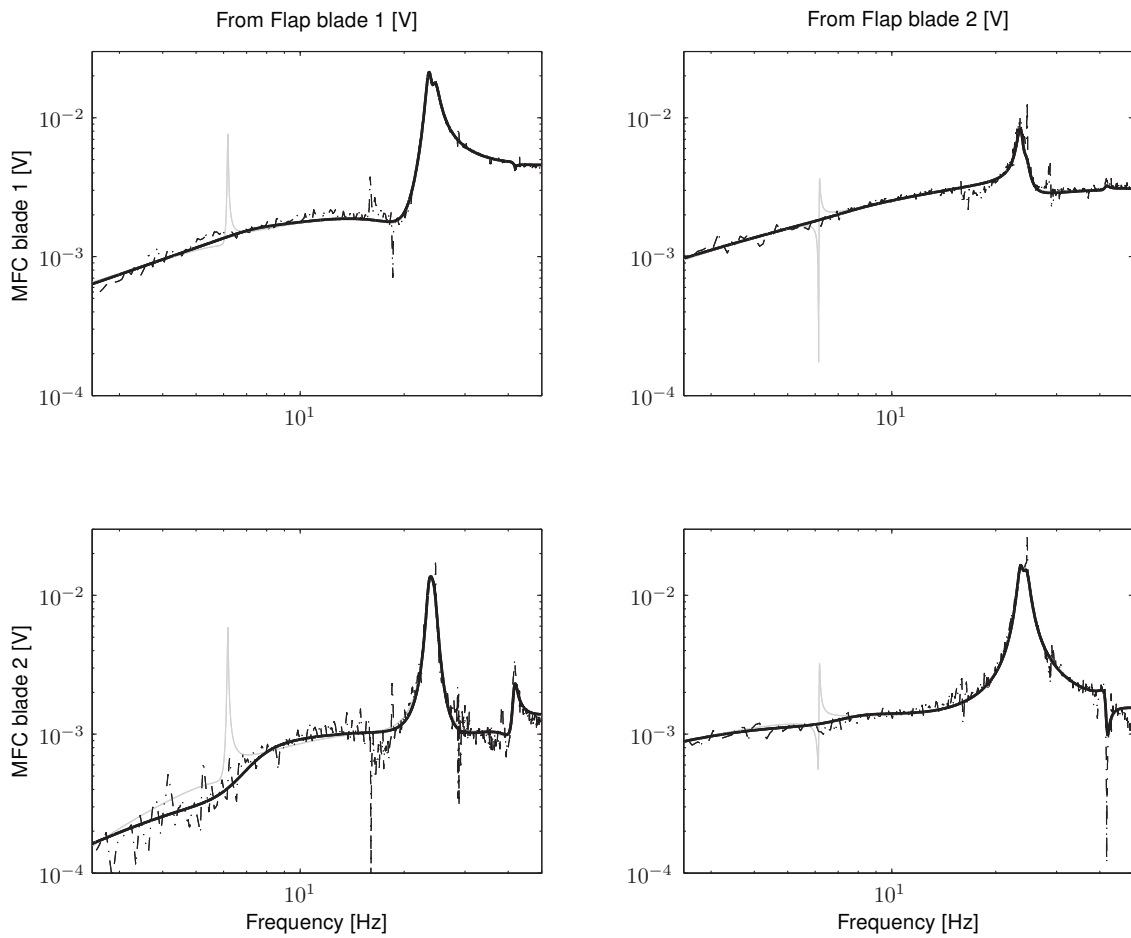


Figure 5: Comparison of the estimated linear model with spectral estimates of the transfer function from the trailing edge actuators to strain measurements at the blade root. The conditions correspond to $\omega = 370$ rpm and $v = 7$ m/s. The gray line corresponds to the models identified without addition of periodic signals.

5.1 Model validation

The quality of the identified models can be assessed in several ways. There is no way to obtain an exact linearised reference model in this case. Therefore, a good start is to compare the identified frequency response functions to the empirical transfer function estimates $\hat{H}_{i \rightarrow j}(e^{j\omega_k})$ based on the FFTs of the input-output data, defined by

$$\hat{H}_{i \rightarrow j}(e^{j\omega_k}) = \frac{Y_j(e^{j\omega_k})}{U_i(e^{j\omega_k})}.$$

The estimates are shown in Figure 5 together with the identified models. On the whole, the results are quite accurate. It is observed that for some cases there are slight differences in the low-frequency behaviour. As a means of cross-validation, the dataset was split up into a $\frac{2}{3}$ part for identification and a $\frac{1}{3}$ part for validation. As a quality measure, the variance-accounted-for (VAF) was used, which gives a measure of how well the variability of the output signal is predicted by the linear model and is expressed as

$$\text{VAF} = \left(1 - \frac{\sum_{j=1}^N (y_j - \hat{y}_j)^2}{\sum_{j=1}^N y_j^2} \right) \times 100\%,$$

where \hat{y} is the output predicted by the identified model. The VAF values were around 95% for both the identification and validation data sets, indicating that a good quality model has been found and that the model does not suffer from over-fitting, in which the model is fitted to the experiment noise. A second test for model quality can be carried out by examining the autocorrelation spectra of the prediction errors $\epsilon_j = y_j - \hat{y}_j$. If the model has truly fitted the input-output data accurately, the prediction error signals should be white noise signals, indicating that all correlation has been removed from the data and all information has been extracted from the signal. In Fig. 6 these spectra are shown together with the 99% confidence bounds and it can be seen that the residual signals are almost uncorrelated. An examination of the spectral content reveals that the correlation still present in the residuals is dominated by some unmodelled periodic components at higher harmonics of the rotor speed.

6 Conclusions

The foregoing sections have demonstrated the potential of subspace system identification for obtaining linear models from operational wind-turbine data. By incorporating the knowledge of the rotor frequency and generating additional input signals, the strong periodic components in the output measurements can be accounted for. The experimental results indicate that the accuracy of a system identification procedure can be improved by adding such periodic signals. The subspace techniques applied here are naturally suited to multivariable systems and the resulting models have been successfully applied

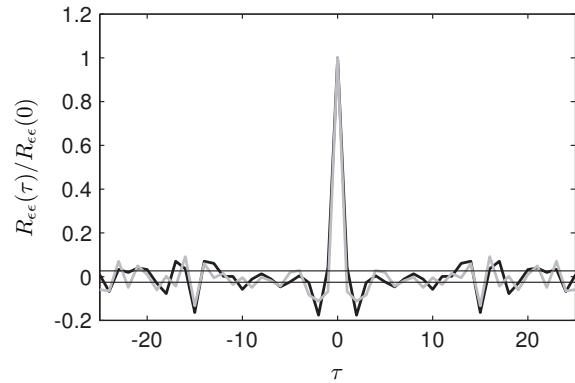


Figure 6: Normalised autocorrelation spectra of the output residual signals between the predicted and true output signals. The concentrated peak at $\tau = 0$ indicates that the signals are almost white.

in model based controller design. Further work will include testing the procedure on the identification of other subsystems of wind turbines, such as reported in [17]. Additionally, we wish to extend the presented methods to techniques that are able to identify locally linear dynamics across the entire operational regime of wind turbines.

References

- [1] D. T. Yen Nakafuji, C. P. van Dam, R. L. Smith, and S. D. Collins. Active load control for airfoils using microtabs. *Journal of Solar Energy Engineering*, 123(4):282–289, 2001.
- [2] N. Troldborg. *Computational Study of the Riso-B1-18 Airfoil Equipped with actively controlled Trailing Edge Flaps*. M.sc thesis, Technical University of Denmark, 2004.
- [3] T. Buhl, M. Gaunaa, and C. Bak. Potential of load reduction using airfoils with variable trailing edge geometry. *Journal of Solar Energy Engineering*, 127(4):503–516, 2005.
- [4] C. P. van Dam, R. Chow, J.R. Zayas, and D. A. Berg. Computational investigations of small deploying tabs and flaps for aerodynamic load control. *Journal of Physics, Conference series: The Science of Making Torque from Wind*, 75(012027), 2007.
- [5] R. Barret. Intelligent rotor blade actuation through directionally attached piezoelectric crystals. In *Proceedings of the 46th Annual forum and technology display*, Washington DC, USA, 1990.
- [6] I. Chopra. Status of application of smart structures technology to rotorcraft systems. *American Helicopter Society*, 45(4):228–252, 2000.

- [7] K.J. Standish and C.P. Van Dam. Computational analysis of a microtab-based aerodynamic load control system for rotor blades. *Journal of the American Helicopter Society*, 50(3):249–258, 2005.
- [8] C. Bak, M. Gaunaa, P.B. Andersen, T. Buhl, P. Hansen, K. Clemmensen, and R. Moeller. Wind tunnel test on wind turbine airfoil with adaptive trailing edge geometry. In *Proceedings of the 45th AIAA Aerospace Sciences Meeting and Exhibit (ASME)*, Reno, USA, 2007.
- [9] J. W. van Wingerden, A. W. Hulskamp, T. Barlas, B. Marrant, G. A. M. van Kuik, D-P. Molenaar, and M. Verhaegen. On the proof of concept of a “smart” wind turbine rotor blade for load alleviation. *Wind Energy*, 11(3):265–280, 2008.
- [10] S. C. Johnson, C. P. van Dam, and D. E. Berg. Active load control techniques for wind turbines. Technical Report SAND08-4809, Sandia National Laboratories, August 2008.
- [11] E. A. Bossanyi. The design of closed loop controllers for wind turbines. *Wind Energy*, 3(3):149–163, 2000.
- [12] E.L. van der Hooft, P. Schaak, and T.G. van Engelen. Wind turbine control algorithms. Technical Report DOWEC-F1W1-EH-030094/0, ECN, 2003.
- [13] F. Lescher, J. Y. Zhao, and A. Martinez. Multiobjective H_2/H_∞ control of a pitch regulated wind turbine for mechanical load reduction. In *Proceedings of the European Wind Energy Conference (EWEC)*, Athens, Greece, 2006.
- [14] M.M. Hand and M.J. Balas. Blade load mitigation control design for a wind turbine operating in the path of vortices. *Wind Energy*, 10(4):339–355, 2007.
- [15] H. F. Veldkamp. *Chances in Wind Energy; A Probabilistic Approach to Wind Turbine Fatigue Design*. PhD dissertation, Delft University of Technology, DUWIND Delft University Wind Energy Research Institute, 10 2006.
- [16] G. E. van Baars and P. M. M. Bongers. Closed loop system identification of an industrial wind turbine system: experiment design and first validation results. In *Proceedings of the 33rd IEEE Conference on Decision and Control, 1994.*, volume 1, pages 625–630 vol.1, Dec 1994.
- [17] M. Iribas and I.-D. Landau. Identification of wind turbines in closed-loop operation in the presence of three-dimensional turbulence wind speed: torque demand to measured generator speed loop. *Wind Energy*, 12(7):660–675, 2009.
- [18] N. E. Goodzeit and M. Q. Phan. System and disturbance identification for feedforward and feedback control applications. *Journal of Guidance, Control and Dynamics*, 23(2):260 – 268, 2000.
- [19] N. E. Goodzeit and M. Q. Phan. System identification in the presence of completely unknown periodic disturbances. *Journal of Guidance, Control and Dynamics*, 23(2):251 – 259, 2000.
- [20] G. E. van Baars, H. Mosterd, and P. M. M. Bongers. Extension to standard system identification of detailed dynamics of a flexible wind turbine system. In *Proceedings of the 32nd IEEE Conference on Decision and Control, 1993.*, pages 3514–3519 vol.4, Dec 1993.
- [21] M. Gevers. Identification for control: From the early achievements to the revival of experiment design. *European Journal of Control*, 11(4-5):335 – 352, 2005.
- [22] P. M. J. Van den Hof and R. J. P. Schrama. Identification and control—closed-loop issues. *Automatica*, 31(12):1751–1770, 1995.
- [23] M. Verhaegen and V. Verdult. *Filtering and System Identification; A Least Squares Approach*. Cambridge University Press, Cambridge, UK, 1st, edition, 2007.
- [24] G. J. van der Veen, J. W. van Wingerden, and M. Verhaegen. Closed-loop MOESP subspace model identification with parametrisable disturbances. Technical report 10-015, Delft Center for Systems and Control, Delft University of Technology, 2010.
- [25] Lennart Ljung. *System Identification: Theory for the User (2nd Edition)*. Prentice Hall PTR, December 1998.
- [26] A. W. Hulskamp, J. W. van Wingerden, T. Barlas, H. Champlaud, G. A. M. van Kuik, H. E. N. Bersee, and M. Verhaegen. Fatigue load alleviation experiments on a scaled wind turbine. In *Proceedings of the 3rd conference, The Science of Making Torque from Wind*, 2010.
- [27] J. W. van Wingerden, A. W. Hulskamp, T. Barlas, I. Houtzager, H. E. N. Bersee, G. A. M. van Kuik, and M. Verhaegen. Two-degree-of-freedom active vibration control of a prototyped “smart” rotor. In *IEEE Transactions on Control System Technology (submitted)*, 2010.